ORIGINAL

Physicomechanical properties and creep behavior of plywood composed of fully and partially heat-treated veneers

Fang-Yu Hsu[1] · Ke-Chang Hung[1] · Jin-Wei Xu[1] · Tung-Lin Wu[2,3] · Jyh-Horng Wu[1]

Abstract

This study investigated the effect of heat-treated veneers on the physicomechanical properties and extended creep behavior of plywood using the stepped isostress method (SSM). The results revealed that the mechanical properties of plywood composed of fully and partially heat-treated veneers were not significantly different from those of the untreated plywood. In addition, the SSM was successfully applied to constructing the plywood creep master curves. The creep resistance of the heat-treated plywood surpassed that of the untreated plywood, especially the $5T_{200}$ plywood, which also exhibited the lowest compliance values of 0.13, 0.14, and 0.15 GPa^{-1} at 5, 10, and 20 years, respectively.

Introduction

Plywood is a manufactured wood-based composite composed of veneers bonded in an odd number of layers, where the grain orientation between adjacent veneers is perpendicular (Ferreira et al. 2017). It is used in furniture production and frame construction and has become increasingly important in the wood market in recent years (Hoadley 2000; Ferreira et al. 2017). Plywood is typically produced from fast-growing forest plantations, giving it undesirable characteristics such as dimensional instability and susceptibility to biological degradation

Fang-Yu Hsu and Ke-Chang Hung have contributed equally to this work.

✉ Jyh-Horng Wu
eric@nchu.edu.tw

1   Department of Forestry, National Chung Hsing University, Taichung 402, Taiwan

2   Department of Wood Science and Design, National Pingtung University of Science and Technology, Pingtung 912, Taiwan

3   College of Technology and Master of Science in Computer Science, University of North America, Fairfax, VA 22033, USA

(particularly with juvenile wood) and therefore, making it unsuitable for outdoor and long-term use (Saka and Ueno 1997; Li et al. 2011; Bekhta et al. 2020). To resolve this issue, plywood veneers require treatment.

Heat treatment is a physical method for wood modification and has received considerable attention in industry due to its cost effectiveness and ecological friendliness (Hill 2006; Kaboorani et al. 2008; Ferreira et al. 2017; Yang et al. 2017; Chien et al. 2018; Auriga et al. 2020). Numerous studies have demonstrated that heat treatment reduces the hygroscopicity (i.e., moisture absorption) (Borrega and Kärenlampi 2010; Ding et al. 2011) and improves the dimensional stability and biological resistance of wood (Kamdem et al. 2002; Bekhta and Niemz 2003; Pétrissans et al. 2003; Gosselink et al. 2004; Yildiz et al. 2006; Gündüz et al. 2008; Hu et al. 2013; Gao et al. 2016; Altgen et al. 2018). Accordingly, heat-treated veneers have enhanced hydrophobicity. In recent years, some studies have investigated the effect of heat treatment on the physicomechanical properties of plywood (Ferreira et al. 2017; Lovrić et al. 2017). Because plywood is often used in construction, the evaluation of creep behavior is crucial. The influence of heat treatment on the creep behavior of plywood remains unclear.

Conducting a full-scale creep test over the service life of the actual material is time-consuming and expensive (Tanks et al. 2017; Hung and Wu 2018; Wei et al. 2020). To reduce the test duration, some short-term accelerated creep tests based on the time–temperature superposition principle (TTSP) and time–stress superposition principle (TSSP), such as the stepped isothermal method (SIM) and stepped isostress method (SSM), have been developed to predict the long-term creep behavior of materials (Hadid et al. 2004; Jones and Clarke 2007; Alwis and Burgoyne 2008; Yeo and Hsuan 2010; Giannopoulos and Burgoyne 2012; Achereiner et al. 2013). According to Hadid et al. (2014) and Huang et al. (2018), the SSM is more suitable for evaluating the creep behavior of materials with low thermal conductivity (e.g., wood and wood-based composites) compared with the SIM because the SSM does not involve elevated temperatures. Therefore, in addition to investigating their physicomechanical properties, a main objective of this study was to predict the extended creep behavior of plywood composed of fully and partially heat-treated veneers through the SSM.

Materials and methods

Materials

Defect-free rotary-cut radiata pine (*Pinus radiata*) veneers (density: 406 ± 30 kg/m^3, moisture content: $9.7 \pm 0.3\%$) with a thickness of 2.2 mm were purchased from Wan Tsai Industry Co., Ltd. (Chiayi, Taiwan). Phenol–formaldehyde resin (PF125; solid content: 46%, viscosity: 757 cps, curing temperature: 150 °C) was supplied by Chang Chun Plastics Co., Ltd. (Hsinchu, Taiwan).

Heat treatment of veneers

The veneers were kept under a continuous flux of nitrogen at a flow rate of 20 mL/min with atmospheric pressure in a hot air circulating oven (JB-27, Prokao, Kaohsiung, Taiwan). The samples were oven-dried at 105 °C for 24 h prior to heat treatment. Subsequently, the samples were heated from 105 °C to the desired temperature (160, 180, 200, and 220 °C), which was maintained for 2 h. The samples were then cooled to room temperature over 40 min.

Preparation of plywood

All veneers with dimensions of 300 mm×300 mm×2.2 mm were conditioned at 20 °C and 65% relative humidity for at least 2 weeks prior to plywood manufacture. Five-ply plywood composed of untreated and heat-treated veneers was fabricated by flat-platen pressing. An adhesive was brushed onto the veneers with a glue amount of 140 g/m^2. The formed plywood panels were cold-pressed at 1.5 MPa for 1 min and then hot-pressed at 160 °C and 1.5 MPa for 7.5 min. In total, 70 panels with a thickness of 10 mm were fabricated, and the veneer layouts in the plywood structure included 5N, 5T, TNTNT, and NTNTN, where N and T represent untreated and heat-treated veneer layers, respectively. Table 1 presents a summary of the five-ply plywood configuration.

Determination of plywood properties

The density, moisture content, and shear bonding strength (warm water soaking Type II) were measured according to the Chinese National Standard CNS 1349 (2014) for plywood. The flexural properties in stress parallel and perpendicular to the grain of the face ply were carried out according to the Standard Test Methods for Testing Structural Panels in Flexure (ASTM D3043-06 2006). The modulus of rupture (MOR) and modulus of elasticity (MOE) of the specimens with dimensions of 290 mm×50 mm×10 mm were determined through the three-point flexural test at a loading speed of 10 mm/min and a span of 240 mm. All samples were conditioned at 20 °C/65% relative humidity for 2 weeks prior to testing. In addition, the

Table 1 Configuration of five-ply plywood specimens

Veneer (Ply)	Plywood			
	5 N	5T$_{xxx}$[a]	NTNTN$_{200}$	TNTNT$_{200}$
Face	Untreated	160–220 °C-treated	Untreated	200 °C-treated
Crossband	Untreated	160–220 °C-treated	200 °C-treated	Untreated
Core	Untreated	160–220 °C-treated	Untreated	200 °C-treated
Crossband	Untreated	160–220 °C-treated	200 °C-treated	Untreated
Back	Untreated	160–220 °C-treated	Untreated	200 °C-treated

[a]Subscript xxx denotes the temperature (160–220 °C) at which the veneer was heat-treated

shear bonding strength of the plywood was determined on samples with dimensions of 80 mm × 25 mm × 10 mm at a tensile speed of 5880 N/min. Prior to the test, the samples were immersed in warm water (60 ± 3 °C) for 3 h, then immersed in cold water until return to room temperature.

Accelerated creep tests

A universal testing machine (Shimadzu AG-10kNX, Tokyo, Japan) was used in the short-term SSM to evaluate the extended creep behavior of the plywood. The creep strain at a reference stress level (σ_{ref}) is provided in Eq. (1):

$$\varepsilon(\sigma_{ref}, t) = \varepsilon(\sigma, t/\alpha_\sigma) \tag{1}$$

where ε is the creep strain as a function of stress and time, σ is the elevated stress, and α_σ is the shift factor. The SSM creep tests were conducted using isostresses between 30% (reference stress level) and 85% of the average breaking load (ABL), with intervals of 5%, 7.5%, 10%, and 12.5% ABL. The dwell time for each isostress was 2 or 3 h. Various SSM testing parameters were used to investigate the differences between the SSM creep tests. In addition, the activation volume was calculated based on the Eyring model below (Eq. 2). This model has been successfully applied to assessing the creep behavior of wood-based composites and estimating the shift factor (α_σ), which shows the following express rate with stress level (Giannopoulos and Burgoyne 2011; Hadid et al. 2014):

$$\log \alpha_\sigma = \log \left(\frac{\dot{\varepsilon}}{\dot{\varepsilon}_r} \right) = \frac{V^*}{2.303kT} \left(\sigma - \sigma_{ref} \right) \tag{2}$$

where $\dot{\varepsilon}$ is the creep rate at the elevated stress level (σ), $\dot{\varepsilon}_r$ is the creep rate at the reference stress level (σ_{ref}), V^* is the activation volume, k is the Boltzmann constant (1.38×10^{-23} J/K), and T is the absolute temperature.

Conventional creep tests

To serve as a basis for comparison with the master curves derived from the accelerated creep tests, a full-scale conventional creep test was conducted at a reference stress level of 30% ABL at 20 °C/65% relative humidity. The mid-span deflection values of the samples were measured and recorded using a linear variable differential transducer over 60 days, and all samples were tested in duplicate.

X-ray diffraction measurement

X-ray diffractograms were obtained with a high-resolution X-ray diffractometer (HRXRD, Bruker D8 SSS, Leipzig, Germany). The diffraction patterns were measured from $2\theta = 2$° to 35° using CuKα_1 radiation at 40 kV and 30 mA. One specimen was used for each determination. Peak separations were measured using PeakFit deconvolution software (Systat Software, Inc., Richmond, CA, USA). After

deconvolution, calculation and comparison of several parameters were possible. The crystallinity index (CrI) and interlayer distance (d_{002}) of the veneers were calculated according to Eqs. (3) and (4), respectively (Poletto et al. 2012):

$$CrI(\%) = \frac{A_{cry}}{A_{cry} + A_{am}} \times 100 \tag{3}$$

$$Interlayer\,distance(d_{002})(nm) = \frac{n\lambda}{2\sin\theta} \times 100 \tag{4}$$

where A_{cry} is sum of crystalline band areas (i.e., the 101, 10ī, and 002 lattice reflections of the cellulose crystallographic form at $2\theta = 14$, 16, and 22°, respectively), A_{am} is the area of the amorphous band at $2\theta = 18°$, n is a constant number, λ is the X-ray wavelength (0.1542 nm), and θ is the Bragg angle corresponding to the 002 lattice.

Analysis of variance

All results were expressed in terms of mean $\pm$ standard deviation (SD). Significant differences were calculated using the Scheffe test, and p values of < 0.05 were considered to be significant.

Results and discussion

Physicomechanical properties of the plywood

The density, moisture content, and mechanical properties of the plywood are summarized in Table 2. The densities of plywood composed of all heat-treated veneers (5 T) were approximately 520–543 kg/m³, which was not statistically different from that of the untreated plywood (5 N, 543 kg/m³). However, the density of NTNTN$_{200}$ plywood, composed of untreated samples and those treated at 200 °C, was 607 kg/m³, which was significantly higher than that of all 5T plywood samples. Similar results were reported by Lovrić et al. (2017). In addition, the moisture content of plywood manufactured from veneers treated at 160 (5T$_{160}$) and 180 °C (5T$_{180}$) was in the range of 11.3–11.8%, not significantly different from that of the untreated plywood (11.2%). However, when the heat treatment temperature reached or exceeded 200 °C, the moisture content decreased considerably. Significantly lower moisture content compared with the untreated plywood was observed in the NTNTN$_{200}$ (7.5%) and TNTNT$_{200}$ (7.3%) specimens. This phenomenon could be attributed to the structural and chemical composition modifications of the veneers through heat treatment, such as the removal of the hemicelluloses and hydroxyl groups and the increase in cellulose crystallinity and thermal cross-linking of lignin (Esteves and Pereira 2009; Windeisen et al. 2009; Tumuluru et al. 2011).

Table 2 Effect of heat treatment temperatures and layouts of veneers on the physicomechanical properties of plywood

Specimen[a]	Density (kg/m^3)	MC (%)	Shear bonding strength		MOR (MPa)		MOE (GPa)	
			Mean (MPa)	Minimum (MPa)	//	⊥	//	⊥
5N	543±18^b	11.2±0.3^a	1.4±0.2^{ab}	1.1	56±3^{ab}	29±1^b	7.2±0.5^{ab}	2.3±0.3^{ab}
5T$_{160}$	523±21^b	11.3±0.2^a	1.7±0.4^a	0.8	55±8^{ab}	29±3^b	5.6±2.4^b	2.1±0.1^b
5T$_{180}$	520±9^b	11.8±0.3^a	1.4±0.3^{ab}	0.9	47±11^b	32±2^{ab}	6.0±0.7^b	2.0±0.3^b
5T$_{200}$	539±18^b	9.7±0.3^b	1.0±0.2^b	0.8	54±7^{ab}	34±7^{ab}	9.3±0.7^a	2.8±0.8^{ab}
5T$_{220}$	543±22^b	9.1±0.1^b	1.1±0.2^b	0.8	42±8^b	26±2^b	7.4±1.0^{ab}	2.5±0.5^{ab}
NTNTN$_{200}$	607±3^a	7.5±0.3^c	1.7±0.6^a	0.7	69±7^a	41±5^a	7.0±0.4^{ab}	2.9±0.3^{ab}
TNTNT$_{200}$	545±7^b	7.3±0.1^c	1.2±0.4^{ab}	0.8	54±3^{ab}	41±4^a	8.2±0.1^{ab}	3.2±0.3^a

Values are represented as mean±SD ($n=5$ for density, MC, and flexural properties; $n=12$ for shear bonding strength). Different superscript letters within a column indicate significant differences at $p < 0.05$

[a]*N*, untreated veneer; *T* heat-treated veneer, *MC*, moisture content, Subscript numbers (160, 180, 200, and 220) denote the temperature (°C) at which the veneer was heat-treated

Table 2 shows the shear bonding strength of all plywood was approximately 1.0–1.7 MPa. The shear bonding strengths of all heat-treated plywood (5T) and hybrid plywood (NTNTN and TNTNT) samples were not significantly different from that of the untreated plywood. Generally, the shear bond strength of plywood decreases with an increase in treatment temperature, because the surface of heat-treated veneer is more hydrophobic and thus, results in a greater decline in bonding performance between veneers (Candana et al. 2012). However, in this study, all plywood composed of fully and partially heat-treated veneers still met the requirements for CNS 1349 Type II plywood (> 0.7 MPa). In addition, the MOR in stress parallel to the face veneer grain (MOR$_{//}$) of the heat-treated plywood (including 5T, NTNTN, and TNTNT) ranged from 42 to 69 MPa, which did not significantly differ from those of the untreated plywood (56 GPa). Similarly, the MOE$_{//}$ values of all heat-treated plywood (5.6–9.3 GPa) were similar to those of the untreated plywood (7.2 GPa). Among all heat-treated plywood, the plywood composed of veneers treated at 200 °C (5T$_{200}$) exhibited the highest MOE$_{//}$ (9.3 GPa). The MOR in stress perpendicular to the face veneer grain (MOR$_\perp$) of the 5T plywood ranged from 26 to 34 MPa, which was not significantly different from that of the untreated plywood (29 MPa). However, the MOR$_\perp$ values of both NTNTN$_{200}$ and TNTNT$_{200}$ were 41 MPa, which was significantly higher than that of the untreated plywood. The MOE$_\perp$ of all the plywood was approximately 2.0–3.2 GPa, and no significant difference was noted between the heat-treated plywood and the untreated plywood.

Determining accelerated creep through the SSM

The extended creep behavior of all plywood was estimated using the SSM. According to the handling process used in studies by Huang et al. (2018) and Hung et al.

(2019), four adjustment steps, including vertical shifting, rescaling, eliminating, and horizontal shifting, were applied to construct the SSM master curve. For brevity, this article mentions only the steps for the untreated plywood. Figure 1a shows the SSM creep curve of the untreated plywood, calculated from the SSM loading sequence at the reference stress level of 30% ABL, with a 7.5% stepwise jump stress and a 2-h dwell time. The immediate strain jump did not cause creep strain during each load change. Vertical shifting was required to eliminate the elastic component in the recorded strain, as Fig. 1b shows. To remove the stress and strain history of previous steps, each creep curve was shifted to the reference stress level (30% ABL) along
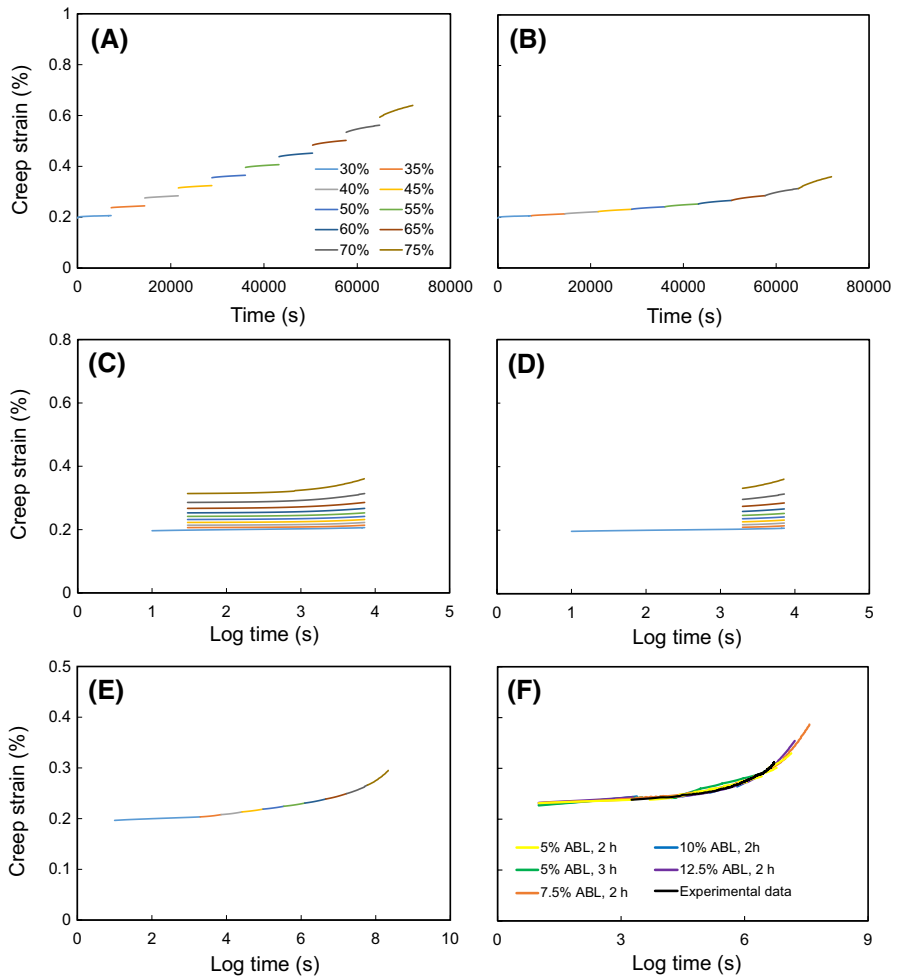

Fig. 1 **a** SSM creep curve of the untreated plywood (reference stress level: 30% ABL; interval stress level: 5% ABL; dwell time: 2 h). SSM test data handling of the SSM test data for untreated plywood: **b** vertical shifting, **c** rescaled creep curves, **d** elimination of the period before the onset time of each stress step, and **e** horizontal shifting. **f** Experimental data and SSM master curves of untreated plywood at different testing parameters on a logarithmic time axis

the logarithmic time axis (Fig. 1c). This rescaling approach was carried out by the modified method that was recommended by Yeo and Hsuan (2009). Subsequently, because it is affected by the stress-level history of the creep strain, the period before the onset time in the primary creep region was eliminated from each individual curve (Fig. 1d). Finally, the rescaled and eliminated individual creep curves were horizontally shifted along the time axis to construct the master curve at the reference stress level (σ_{ref}). The magnitude of this shift factor $\log(\alpha_\sigma)$ is a function of the stress level and is calculated using the Eyring equation. The trend of the SSM shift factors in terms of creep stress was found to fit the Eyring model. Figure 1e shows the final smooth master curve of the untreated plywood. None of the master curves were affected by stress increments and dwell times, and fitted well with the 60-day experimental data under 30% ABL (Fig. 1f). Therefore, the SSM master curve could be used to predict the long-term creep behavior of the untreated plywood.

Similarly, as Fig. 2 shows, the master curves of all the plywood composed of heat-treated veneers also fitted well with their experimental creep data, suggesting that the SSM is suitable for and applicable to the evaluation and comparison of creep behaviors of various types of plywood. Figure 3 shows the shift factor data of stress levels from the SSM testing parameters in terms of the accelerated creep stress at the reference stress level of 30% ABL. The shift factor data in this plot are almost in a straight line and show low experimental scatter, and all linear regression coefficients of determination (R^2) are greater than 0.90. This result was similar to those from previous studies (Yeo and Hsuan 2009; Giannopoulos and Burgoyne 2012; Hung et al. 2019), which indicated that different SSM testing parameters had no effect on the construction of master curves for polymeric and wood-based materials. This suggests that the same creep mechanism was active for each stress sequence, which in turn proved that the time–stress superposition principle could be applied to construction of the creep master curve. The activation volume (V^*) was calculated from the linear slope based on the Eyring model (Eq. (4)). The V^* values of all the heat-treated plywood (5T) (0.793–1.010 nm^3) veneers were lower than those of the untreated veneers (1.134 nm^3), except in the case of $5T_{180}$ (1.421 nm^3). The V^* values of $NTNTN_{200}$ and $TNTNT_{200}$ were 1.685 and 0.926 nm^3, respectively. According to Gao et al. (2015), the activation volume corresponds to chain slippage within crystalline lamellae in the lamellar clusters. The reduction in activation volume can be attributed to the decrease in the interlayer distance between the cellulose crystalline lamellae of the composed veneers.

An X-ray diffractometer was used to determine the interlayer distance (d_{002}) and crystallinity index of the veneers before and after heat treatment. Figure 4 shows the evolution of X-ray diffraction patterns of the untreated veneers and veneers treated at different temperatures. For the untreated veneers, two diffraction peaks were observed at $2\theta = 15°$ and $22°$, and the CrI was 34%. The first peak was attributed to the 101 and 10ī planes of the crystal lattice and the second peak corresponded to the reflection of the 002 plane of the native cellulose lattice. The CrI of the veneers increased with an increase in heat treatment temperatures; at 160, 180, 200, and 220 °C, their CrI values were 38%, 39%, 44%, and 47%, respectively. This trend is approximately consistent with the $MOE_{//}$ changes shown in Table 2. However, the d_{002} of the veneers treated at 180 °C (0.399 nm)
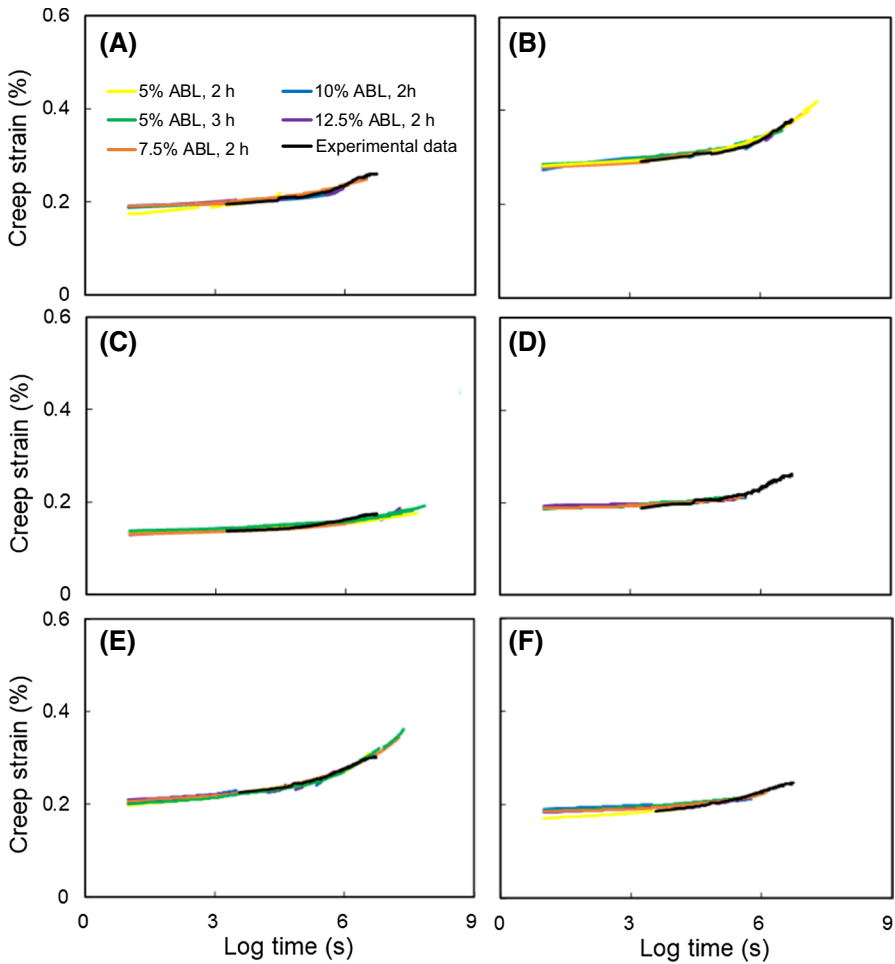
Fig. 2 SSM master curves and experimental curves of plywood composed of fully and partially heat-treated veneers. **a** $5T_{160}$, **b** $5T_{180}$, **c** $5T_{200}$, **d** $5T_{220}$, **e** $NTNTN_{200}$, and **f** $TNTNT_{200}$

was slightly larger than that of other heat-treated veneers (0.398 nm). This trend is similar to that of the activation volume changes, but further research is warranted to determine the exact reasons for the lower activation volume of the heat-treated plywood, especially that of $NTNTN_{200}$.

SSM-predicted creep curves

To assess the changes in the flexural strength of the specimens, creep compliance ($J(t)$) was used to measure the time-dependent creep, which is given in Eq. (5) (Chevali et al. 2009):
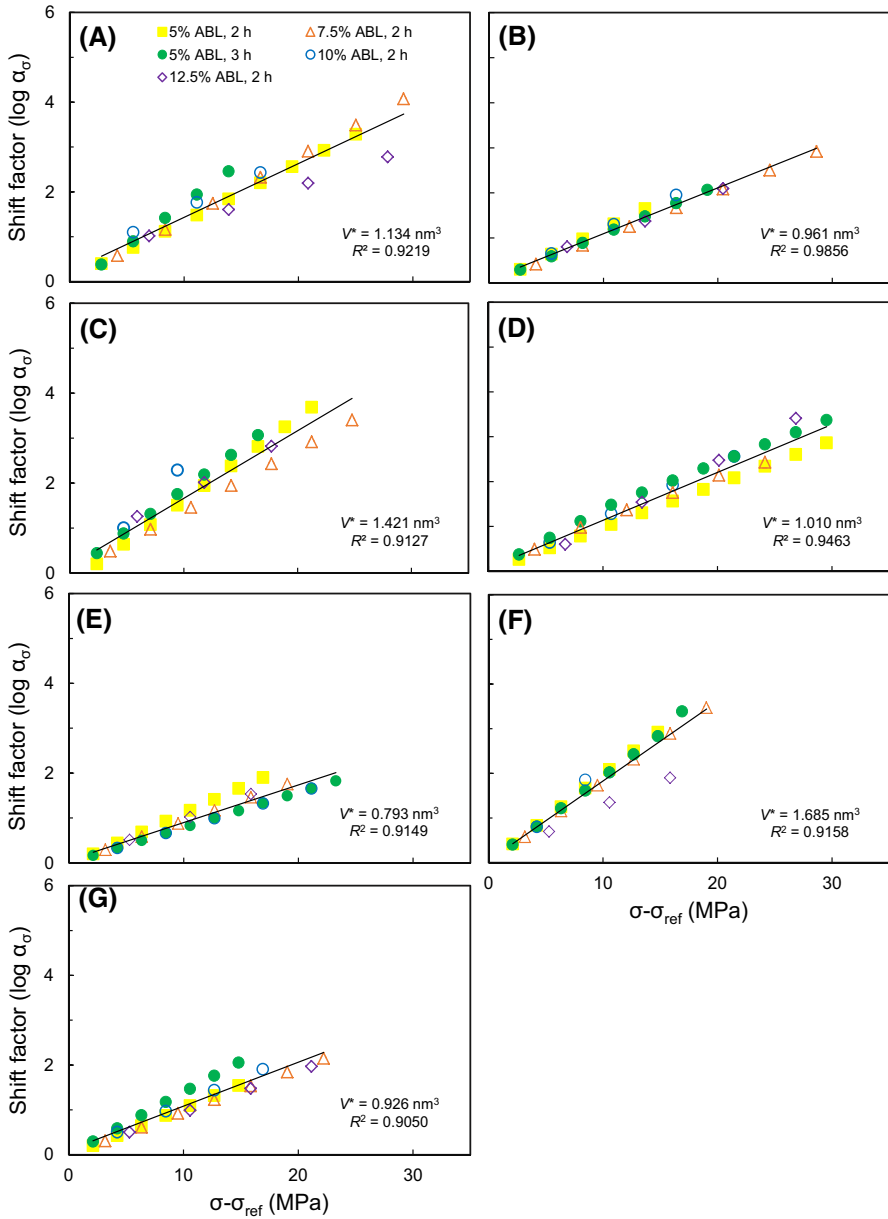
Fig. 3 Typical Eyring plots of plywood composed of untreated and heat-treated veneers at different SSM testing parameters under a reference stress level of 30% ABL. **a** 5 N, **b** 5T$_{160}$, **c** 5T$_{180}$, **d** 5T$_{200}$, **e** 5T$_{220}$, **f** NTNTN$_{200}$, and **g** TNTNT$_{200}$
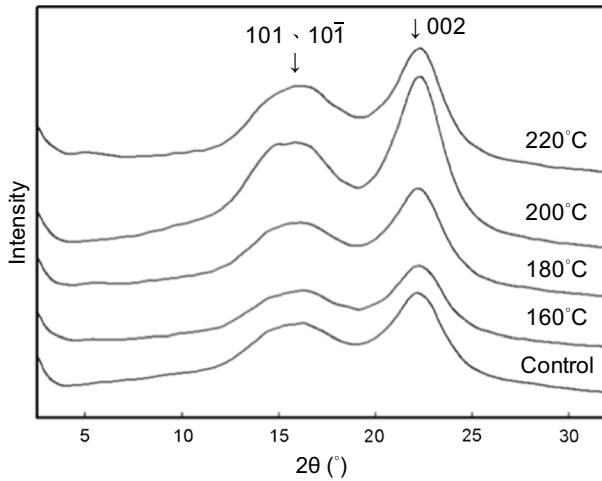
Fig. 4 X-ray diffraction spectra of veneers treated at different temperatures

$$J(t)\left(\mathrm{MPa}^{-1}\right) = 4bh^3 D(t)/PL^3 \tag{5}$$

where b is the width of the specimen, h is the thickness of the specimen, $D(t)$ is the time-dependent deflection (deformation), t is the elapsed time, P is the applied load, and L is the span length. The SSM-predicted creep compliance master curves of plywood composed of various heat-treated veneers on a normal time scale (Fig. 5) show that except for $5T_{180}$, all heat-treated plywood had lower creep compliance than untreated plywood (5N) during creep. Many models have been used to fit the creep curves for wood and wood-based materials such as Burger's
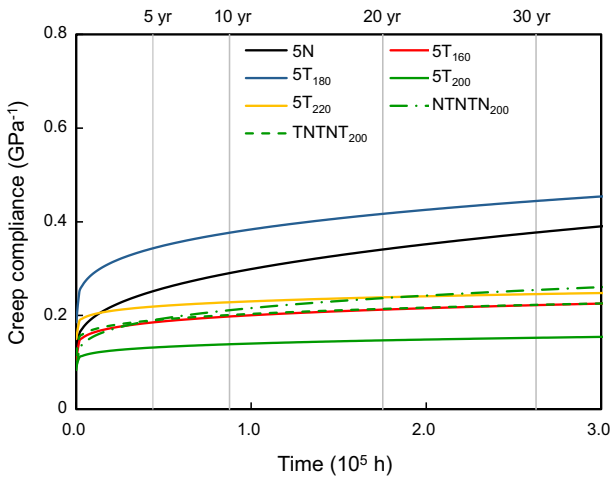

Fig. 5 SSM-predicted creep data of plywood composed of fully and partially heat-treated veneers at a reference stress level of 30% ABL

model and Findley power law model. Of these, the Findley power law model is not only simpler to use, but also suitable for fitting the creep curves of wood and wood-based composites (Yang et al. 2017; Huang et al. 2018; Hung and Wu 2018; Hung et al. 2019). Accordingly, in the present study, curve fitting was performed using the Findley power law equation with three parameters (Eq. 6):

$$S(t) = S_0 + at^b \tag{6}$$

where $S(t)$ is the time-dependent compliance value, S_0 is the instantaneous elastic compliance value, a and b are constant values, and t is elapsed time. Table 3 summarizes the resulting fitted parameters and shows that the R^2 values of all plywood were greater than 0.98.

Table 3 presents the instantaneous elastic compliance (S_0) and the predicted time-dependent compliance values ($S(t)$) of all the samples over 5–30 years. Accordingly, the S_0 value of untreated plywood was 0.123 GPa^{-1}, and the S_0 value of plywood composed of fully (5T) and partially (NTNTN$_{200}$ and TNTNT$_{200}$) heat-treated veneers ranged from 0.084 to 0.186 GPa^{-1}. The predicted compliance values of the 5N plywood were 0.25, 0.29, 0.34, and 0.38 GPa^{-1} at 5, 10, 20, and 30 years, respectively. The compliance values of the plywood composed of various heat-treated veneers considerably declined over a 30-year period compared with untreated plywood, except for 5T$_{180}$. The 5T$_{200}$ plywood had the lowest compliance values of 0.13, 0.14, 0.15, and 0.15 GPa^{-1} at 5, 10, 20, and 30 years, respectively.

Long-term improvement in the creep resistance (ICR) of the plywood was calculated according to Eq. (7):

Table 3 Predicted creep compliance of plywood composed of fully and partially heat-treated veneers

Specimen[a]	S_0 (GPa^{-1})	a	b	R^2	$S(t)$ (GPa^{-1})				ICR (%)			
					Time (years)				Time (years)			
					5	10	20	30	5	10	20	30
5N	0.123	0.0022	0.38	0.997	0.25	0.29	0.34	0.38	–	–	–	–
5T$_{160}$	0.105	0.0085	0.21	0.995	0.19	0.20	0.21	0.22	26	32	38	41
5T$_{180}$	0.186	0.0082	0.28	0.999	0.34	0.38	0.42	0.44	−36	−0	−22	−8
5T$_{200}$	0.092	0.0032	0.24	0.987	0.13	0.14	0.15	0.15	48	2	57	60
5T$_{220}$	0.150	0.0099	0.18	0.982	0.22	0.23	0.24	0.25	13	21	30	35
NTNTN$_{200}$	0.084	0.0063	0.27	0.997	0.21	0.24	0.25	0.21	25	27	30	33
TNTNT$_{200}$	0.115	0.0083	0.21	0.996	0.20	0.21	0.22	0.20	25	31	37	41

$S(t) = S_0 + at^b$, where $S(t)$ is the time-dependent compliance value, S_0 is the instantaneous elastic compliance value, and a and b are constant values

[a]N untreated veneer, T heat-treated veneer. Subscript numbers (160, 180, 200, and 220) denote the temperature (°C) at which the veneer was treated

$$\text{ICR}(\%) = \left[1 - \frac{S(t)_h}{S(t)_u} \right] \times 100 \qquad (7)$$

where $S(t)_u$ and $S(t)_h$ are the time-dependent compliance values of plywood composed of untreated and heat-treated veneers, respectively. As Table 3 shows, $5T_{200}$ exhibited the highest ICR values of 48%, 52%, 57%, and 60% at 5, 10, 20, and 30 years, respectively. By contrast, the creep resistance of $5T_{180}$ decreased over a 30-year period. These results suggest that the long-term creep resistance of plywood would be improved through heat treatment of veneers, except for treatment at 180 °C.

Conclusion

The moisture content of plywood composed of veneers fully and partially heat-treated at 200 °C ($5T_{200}$, $NTNTN_{200}$, and $TNTNT_{200}$) was lower than that of the untreated plywood, but no significant difference was noted between mechanical properties of the heat-treated plywood and the untreated plywood. In addition, the creep master curve predicted by SSM showed a good fit with the 60-day experimental data of untreated and heat-treated plywood, and the testing parameters had no effect on the construction of master curves. These results demonstrated that the same creep mechanism was active for each stress sequence and SSM could be used to evaluate the long-term creep behavior of plywood. Furthermore, the shift factor data on the Eyring plots were almost in a straight line and showed low experimental scatter. As calculated from the linear slope of the Eyring plots, the activation volume of the heat-treated plywood (0.793–1.010 nm^3) was lower than that of the untreated plywood (1.134 nm^3), except for the plywood composed of veneers treated at 180 °C ($5T_{180}$, 1.421 nm^3). The compliance values of plywood composed of fully (5 T) and partially ($NTNTN_{200}$ and $TNTNT_{200}$) heat-treated veneers considerably declined over a 30-year period, except for $5T_{180}$. The plywood composed of veneers treated at 200 °C ($5T_{200}$) exhibited a 60% improvement in creep resistance and had the highest creep resistance overall.

Compliance with ethical standards

Conflict of interest The authors declare that there is no conflict of interest regarding the publication of this paper.

References

Achereiner F, Engelsing K, Bastian M, Heidemeyer P (2013) Accelerated creep testing of polymers using the stepped isothermal method. Polym Test 32:447–454. https://doi.org/10.1016/j.polymertesting.2013.01.014

Altgen M, Willems W, Hosseinpourpia R, Rautkari L (2018) Hydroxyl accessibility and dimensional changes of Scots pine sapwood affected by alterations in the cell wall ultrastructure during

heat-treatment. Polym Degrad Stabil 152:244–252. https://doi.org/10.1016/j.polymdegradstab.2018.05.005

Alwis KGNC, Burgoyne CJ (2008) Accelerated creep testing for aramid fibres using the stepped isothermal method. J Mater Sci 43:4789–4800. https://doi.org/10.1007/s10853-008-2676-0

ASTM D3043-06 (2006) Standard test methods for structural panels in flexure. ASTM International, West Conshohocken, PA, USA

Auriga R, Gumowska A, Szymanowski K, Wronka A, Robles E, Ocipka P, Kowaluk G (2020) Performance properties of plywood composites reinforced with carbon fibers. Compos Struct 248:112533. https://doi.org/10.1016/j.compstruct.2020.112533

Bekhta P, Niemz P (2003) Effect of high temperature on the change in color, dimensional stability and mechanical properties of spruce wood. Holzforschung 57:539–546. https://doi.org/10.1515/HF.2003.080

Bekhta P, Salca EA, Lunguleasa A (2020) Some properties of plywood panels manufactured from combinations of thermally densified and non-densified veneers of different thicknesses in one structure. J Build Eng 29:101116. https://doi.org/10.1016/j.jobe.2019.101116

Borrega M, Kärenlampi PP (2010) Hygroscopicity of heat-treatend Norway spruce (*Picea abies*) wood. Eur J Wood Prod 68:233–235. https://doi.org/10.1007/s00107-009-0371-8

Candana Z, Büyüksarı U, Korkut S, Unsal O, Çakıcıer N (2012) Wettability and surface roughness of thermally modified plywood panels. Ind Crop Prod 36:434–436. https://doi.org/10.1016/j.indcrop.2011.10.010

Chevali VS, Dean DR, Janowski GM (2009) Flexural creep behavior of discontinuous thermoplastic composites: Non-linear viscoelastic modeling and time–temperature–stress superposition. Compos Part A Appl S 40:870–877. https://doi.org/10.1016/j.compositesa.2009.04.012

Chien Y-C, Yang T-C, Hung K-C, Li C-C, Xu J-W, Wu J-H (2018) Effects of heat treatment on the chemical compositions and thermal decomposition kinetics of Japanese cedar and beech wood. Polym Degrad Stabil 158:365–378. https://doi.org/10.1016/j.polymdegradstab.2018.11.003

Chinese National Standard CNS 1349 (2014) Plywood. Bureau of Standards, Metrology and Inspection, Taipei, Taiwan

Ding T, Gu L, Li T (2011) Influence of steam pressure on physical and mechanical properties of heat-treated Mongolian pine lumber. Eur J Wood Prod 69:121–126. https://doi.org/10.1007/s00107-009-0406-1

Esteves BM, Pereira HM (2009) Wood modification by heat treatment: a review. BioResources 4:370–404

Ferreira BS, Silva JVF, Campos CI (2017) Static bending strength of heat-treated and chromated copper arsenate-treated plywood. BioResources 12:6276–6282. https://doi.org/10.15376/biores.12.3.6276-6282

Gao R, Kuriyagawa M, Nitta K-H, He X, Liu B (2015) Structural interpretation of Eyring activation parameters for tensile yielding behavior of isotactic polypropylene solids. J Macromol Sci B 54:1196–1210. https://doi.org/10.1080/00222348.2015.1079088

Gao J, Kim JS, Terziev N, Daniel G (2016) Decay resistance of softwoods and hardwoods thermally modified by the Thermovouto type thermos-vacuum process to brown rot and white rot fungi. Holzforschung 70:877–884. https://doi.org/10.1515/hf-2015-0244

Giannopoulos IP, Burgoyne CJ (2011) Prediction of the long-term behaviour of high modulus fibres using the stepped isostress method (SSM). J Mater Sci 46:7660–7671. https://doi.org/10.1007/s10853-011-5743-x

Giannopoulos IP, Burgoyne CJ (2012) Accelerated and real-time creep and creep-rupture results for aramid fibers. J Appl Polym Sci 125:3856–3870. https://doi.org/10.1002/app.36707

Gosselink RJA, Krosse AMA, van der Putten JC, van der Kolk JC, de Klerk-Engels B, van Dam JEG (2004) Wood preservation by low-temperature carbonisation. Ind Crop Prod 19:3–12. https://doi.org/10.1016/S0926-6690(03)00037-2

Gündüz G, Korkut S, Korkut DS (2008) The effects of heat treatment on physical and technological properties and surface roughness of Camiyani Black Pine (*Pinus nigra* Arn. subsp. *pallasiana* var. *pallasiana*) wood. Bioresour Technol 99:2275–2280. https://doi.org/10.1016/j.biortech.2007.05.015

Hadid M, Rechak S, Tati A (2004) Long-term bending creep behavior prediction of injection molded composite using stress-time correspondence principle. Mater Sci Eng A Struct 385:54–58. https://doi.org/10.1016/j.msea.2004.04.023

Hadid M, Guerira B, Bahri M, Zouani A (2014) Assessment of the stepped isostress method in the prediction of long term creep of thermoplastics. Polym Test 34:113–119. https://doi.org/10.1016/j.polymertesting.2014.01.003

Hill CAS (2006) Wood modification: chemical, thermal and other process. Wiley, Chichester

Hoadley RB (2000) Understanding wood: a craftsman's guide to wood technology. The Taunton Press, Newtown

Hu C, Juifen G, Zhou J, Xiao M, Yi Z (2013) Effect of the thickness of the heat treated wood specimen on water-soluble extractives and mechanical properties of Merbau heartwood. BioResources 8:603–611. https://doi.org/10.15376/biores.8.1.603-611

Huang CW, Yang TC, Wu TL, Hung KC, Wu JH (2018) Effects of maleated polypropylene content on the extended creep behavior of wood polypropylene composites using the stepped isothermal method and the stepped isostress method. Wood Sci Technol 52:1313–1330. https://doi.org/10.1007/s00226-018-1037-7

Hung K-C, Wu J-H (2018) Effect of SiO_2 content on the extended creep behavior of SiO_2-basedwood-inorganic composites derived *via* the sol-gel process using the stepped isostress method. Polymers 10:409–420. https://doi.org/10.3390/polym10040409

Hung K-C, Wu T-L, Wu J-H (2019) Long-term creep behavior prediction of sol-gel derived SiO_2- and TiO_2-wood composites using the stepped isostress method. Polymers 11:1215–1226. https://doi.org/10.3390/polym11071215

Jones CJFP, Clarke D (2007) The residual strength of geosynthetic reinforcement subjected to accelerated creep testing and simulated seismic events. Geotext Geomembr 25:155–169. https://doi.org/10.1016/j.geotexmem.2006.12.004

Kaboorani A, Faezipour M, Ebrahimi G (2008) Feasibility of using heat treated wood in wood/thermoplastic composites. J Reinf Plast Comp 27:1689–1699. https://doi.org/10.1177/0731684407084207

Kamdem DP, Pizzi A, Jermannaud A (2002) Durability of heat-treated wood. Eur J Wood Prod 60:1–6. https://doi.org/10.1007/s00107-001-0261-1

Li YF, Dong XY, Liu YX, Li J, Wang FH (2011) Improvement of decay resistance of wood *via* combination treatment on wood cell wall: swell-bonding with maleic anhydride and graft copolymerization with glycidyl methacrylate and methyl methacrylate. Int Biodeter Biodegr 67:1087–1094. https://doi.org/10.1016/j.ibiod.2011.08.009

Lovrić A, Zdravković V, Popadić R, Milić G (2017) Properties of plywood boards composed of thermally modified and non-modified poplar veneer. BioResources 12:8581–8594. https://doi.org/10.15376/biores.12.4.8581-8594

Pétrissans M, Gérardin P, El bakali I, Serraj M (2003) Wettability of heat-treated wood. Holzforschung 57:301–307. https://doi.org/10.1515/HF.2003.045

Poletto M, Zattera AJ, Forte MMC, Santana RMC (2012) Thermal decomposition of wood: influence of wood components and cellulose crystallite size. Bioresour Technol 109:148–153. https://doi.org/10.1016/j.biortech.2011.11.122

Saka S, Ueno T (1997) Several SiO_2 wood-inorganic composites and their fire-resisting properties. Wood Sci Technol 31:457–466. https://doi.org/10.1007/BF00702568

Tanks JD, Rader KE, Sharp SR (2017) Accelerated creep and creep-rupture testing of transverse unidirectional carbon/epoxy lamina based on the stepped isostress method. Compos Struct 159:455–462. https://doi.org/10.1016/j.compstruct.2016.09.096

Tumuluru JS, Sokhansanj S, Hess JR, Wright CT, Boardman RD (2011) A review on biomass torrefaction process and product properties for energy applications. Ind Biotechnol 7:384–401. https://doi.org/10.1089/ind.2011.7.384

Wei Y, Zhao K, Hang C, Si C, Ding M (2020) Experimental study on the creep behavior of recombinant bamboo. J Renew Mater 8(3):251–273. https://doi.org/10.32604/jrm.2020.08779

Windeisen E, Bächle H, Zimmer B, Wegener G (2009) Relations between chemical changes and mechanical properties of thermally treated wood. Holzforschung 63:773–778. https://doi.org/10.1515/HF.2009.084

Yang T-C, Chien Y-C, Wu T-L, Hung K-C, Wu J-H (2017) Effects of heat-treated wood particles on the physico-mechanical properties and extended creep behavior of wood/recycled-HDPE composites using the time–temperature superposition principle. Materials 10:365–378. https://doi.org/10.3390/ma10040365

Yeo SS, Hsuan YG (2009) Service life prediction of polymeric materials: global perspectives. Springer, New York

Yeo SS, Hsuan YG (2010) Evaluation of creep behavior of high density polyethylene and polyethylene-terephthalate geogrids. Geotext Geomembr 28:409–421. https://doi.org/10.1016/j.geotexmem.2009.12.003

Yildiz S, Gezer ED, Yildiz UC (2006) Mechanical and chemical behavior of spruce wood modified by heat. Build Environ 41:1762–1766. https://doi.org/10.1016/j.buildenv.2005.07.017

Publisher's Note Springer Nature remains neutral with regard to jurisdictional claims in published maps and institutional affiliations.